Princeton Plasma Physics Laboratory

PPPL- 4707

PPPL- 4707

Sensitivity to Error Fields in NSTX High Beta Plasmas

Jong-Kyu Park, Jonathan E. Menard, Stefan P. Gerhardt, Richard J. Buttery,
Steve A. Sabbagh, Ronald E. Bell and Benoit P. LeBlanc

November, 2011

Prepared for the U.S. Department of Energy under Contract DE-AC02-09CH11466.

Princeton Plasma Physics Laboratory
Report Disclaimers

Full Legal Disclaimer

Trademark Disclaimer

PPPL Report Availability

Princeton Plasma Physics Laboratory:

http://www.pppl.gov/techreports.cfm

Office of Scientific and Technical Information (OSTI):

http://www.osti.gov/bridge

Related Links:

U.S. Department of Energy

Office of Scientific and Technical Information

Fusion Links

Sensitivity to Error Fields in NSTX High β Plasmas

Jong-Kyu Park,[1] Jonathan E. Menard,[1] Stefan P. Gerhardt,[1] Richard J. Buttery,[2] Steve A. Sabbagh,[3] Ronald E. Bell,[1] and Benoit P. LeBlanc[1]

[1]*Princeton Plasma Physics Laboratory, Princeton, New Jersey, NJ 08543*

[2]*General Atomics, San Diego, CA 92186*

[3]*Department of Applied Physics and Applied Mathematics, Columbia University, New York, NY 10027*

(Dated: November 3, 2011)

Abstract

It was found that error field threshold decreases for high β in NSTX, although the density correlation in conventional threshold scaling implies the threshold would increase since higher β plasmas in our study have higher plasma density. This greater sensitivity to error field in higher β plasmas is due to error field amplification by plasmas. When the effect of amplification is included with ideal plasma response calculations, the conventional density correlation can be restored and threshold scaling becomes more consistent with low β plasmas. However, it was also found that the threshold can be significantly changed depending on plasma rotation. When plasma rotation was reduced by non-resonant magnetic braking, the further increase of sensitivity to error field was observed.

I. INTRODUCTION

Tokamaks are almost axisymmetric, but small deviations in magnetic field exist intrinsically due to imperfections in primary magnets and surrounding conductors. It is essential to control these small deviations since they can greatly change tokamak performance. One of the worst effects by non-axisymmetric *error* field is the plasma locking [1–9], which often eventually causes a plasma disruption. Error field correction therefore typically aims at the reduction or compensation of error field using non-axisymmetric control coils, to the level below a threshold where a locking may take place. Understanding of error field threshold, or often equivalently locking threshold, is thus prerequisite to achieve reliable error field correction.

Locking is associated with magnetic islands at the rational surfaces. It is understood of the sudden opening of islands when the electromagnetic torque by error field can overcome the compensating viscous torque [10, 11], but the possible dynamics are highly complex depending on plasma parameters [12]. Nonetheless the empirical trend for error field threshold has been found in relatively simplified fashion. The most common observation is that error field threshold increases almost linearly with plasma density. Accordingly, error field has been considered as a more important topic in Ohmic plasmas, which have low β and low plasma density and thus can be more sensitive to error field. It has also been noted that ITER will have a long Ohmic period before the flat-top of plasma currents. By these reasons, the study of error field threshold has been focused on Ohmic plasmas in many devices, including DIII-D [5, 9], CMOD [6], COMPASS-D [3], JET [4], MAST [7], and NSTX [8]. In recent years, however, error field threshold in high β plasmas also became an important issue, along with new prediction for large plasma amplification of error field in high β plasmas.

Understanding of error field physics has been greatly improved these days, especially on the effects of plasma response to error field [13–16]. It has been shown that plasma response can largely change the field penetration by distorting the spectrum of error field and also by changing the amplitude of error field. The change in the field amplitude is expected large especially in high β plasmas through their greater amplification of the externally given magnetic field [16, 17]. That is, the actual driving field of locking can be higher than the external field, and thus the favorable density scaling in high density can be degraded and

become unfavorable by increased $\beta \propto nT$. Therefore, the study of error field threshold should be extended and thoroughly investigated in high β plasmas as well as in low β plasmas.

One important question prior to the study is if error field threshold in high β, which often includes significant input torques by axillary heating, can be defined in the same way for low β and Ohmic plasmas. In Ohmic plasmas, error field threshold is defined as a critical amplitude in the non-axisymmetric components of the magnetic field to produce a locking. Since many observations indicate that locking occurs by $(m, n) = (2, 1)$ islands at the $q = 2/1$ resonant surface [3–8], the resonant field δB_{21} driving $(2, 1)$ magnetic islands naturally becomes the measure of threshold. This is a strong reduction of complexity in error field study, from the fully three-dimensional nature of non-axisymmetric magnetic field to mere a scalar quantity [9]. The relevance of this method in high β should be considered, by investigating the main cause of disruption in the presence of error field.

This study found that error field can disrupt high β plasmas with certain threshold. Large $n = 1$ signals were always observed before disruptions and thus $n = 1$ MHD events were obviously involved. This is not by unstable Kink or Resistive Wall Mode (RWM) [18–20], as β_N in this study was not high enough to reach the no-wall stability limit. Our speculation is that this is by locking at the $q = 2/1$ resonant surface, similar to Ohmic plasmas, since the evolution of electron temperature and rotation profiles indicate island opening at $q = 2/1$. Figure 1 is an example, as one can see the temperature flattening at the $q = 2/1$ surface, and more evidently, the rotation decreases and is almost locked to the frame of external error field at the $q = 2/1$ surface.

This clear picture was in fact not always easy to see in our experiments, due to the short period of time between locking and disruption compared to time resolution in CHERS and TS measurements, and also due to injected toroidal torques by NBI. Injected torques enable plasmas to maintain larger shielding currents, but islands would be bigger when they open due to large shielding currents. Note in general that an island size at $q = m/n$ is proportional to $\sqrt{\delta B_{mn}}$, where the resonant field δB_{mn} driving the island is proportional to dissipated shielding currents. If $(2, 1)$ islands are big enough to reach to adjacent $n = 1$ rational surfaces, they can affect other $(m > 2, n = 1)$ islands as soon as they open and thus possibly cause the wide collapse of temperature profiles in the region $q > 2$, as occasionally found in our study. Also in this case, rotation can be more resilient for a change due to injected torques and begin to collapse from the outside where injected torques are relatively

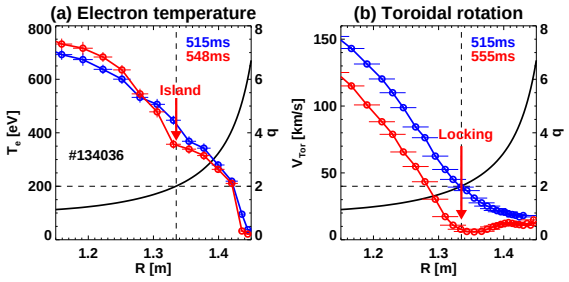

FIG. 1. Example of profile evolutions of (a) electron temperature and (b) toroidal rotation, during a locking by external field in NSTX high-β plasmas. One can see the temperature flattening and the rotation decrease at the $q = 2/1$ surface when time approaches to an actual locking $\sim 550ms$. These measurements imply that the $(m, n) = (2, 1)$ resonant field driving islands should also be the primary measure of error field threshold.

small. In such cases, it is not clear what causes the collapse of discharges. However, this paper will assume that $(2, 1)$ islands are still the fundamental drive of locking and disruption, based on many other examples as illustrated in Figure 1, and therefore error field threshold will be defined consistently across low β and high β plasmas.

The rest of the paper is organized as follows. Section 2 will describe experimental details and observations, which show clearly the increased sensitivity of plasmas to error field in higher β. Section 3 will describe ideal plasma calculations to explain experiments and will demonstrate the successful scaling of error field threshold across low β and high β plasmas. Section 4 will discuss effects by plasma rotation on error field threshold and Section 5 will summarize the paper.

II. EXPERIMENT: ERROR FIELD APPLICATION TO HIGH-BETA NSTX PLASMAS

This study targeted the strongly shaped and high β plasmas in NSTX as shown in Figure 2. Plasmas are diverted with a lower single null with the aspect ratio $A \sim 1.4$, the elongation $\kappa \sim 2.3$, the triangularity $\delta_{up} \sim 0.4$ and $\delta_{down} \sim 0.8$, the safety factor $q_{95} = 8 \sim 10$, and the plasma $\beta_N = 3 \sim 4 < \beta_{N,no-wall}$. The $n = 1$ error field is produced by the 6-toroidal array of Error Field Correction (EFC) [8, 21] coils at the midplane as shown in the 2D and 3D schematics in Figure 2. By changing currents in EFC coils, one can measure the critical

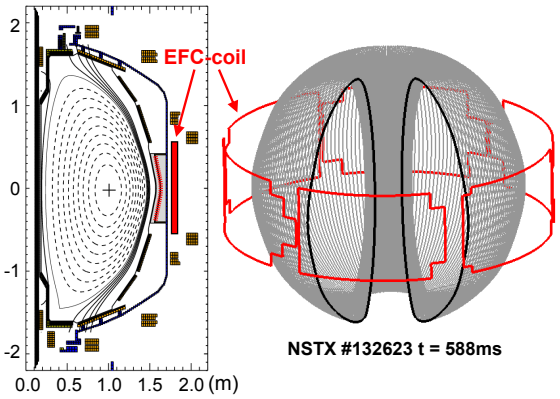

FIG. 2. An example of reconstructed target equilibria in NSTX using LRDFIT (LR circuit model with Data FITting capabilities), which gives a reconstructed Grad-Shafranov equilibrium constrained by magnetic measurements, MSE, T_e-isoflux, and toroidal rotation, including vessel eddy current effects [22]. The poloidal locations of EFC coils in are shown on the left in 2D and on the right in 3D. EFC coils are all located at the midplane. There are 6 coils along the toroidal direction and the $n = 1$ field can be produced with almost an arbitrary toroidal phase.

amplitude and the threshold at locking.

Error field threshold can be studied either by changing applied coil currents, as done in our study, or by changing plasma parameters while holding the applied coil currents. In fact, none of these methods is perfect in NSTX high β targets due to continuous change of several plasma parameters such as plasma density and also due to dynamic change of the intrinsic error field [8]. The change in coil currents are faster than the changes in parameters and intrinsic errors during the flat-top, but it is still necessary to estimate each dynamic parameter at each time just before a locking. The effects by intrinsic errors are small but not ignorable, as will be illustrated later.

Figure 3 shows a typical sequence of our experiments in time. The same plasma current in (a), $I_P = 900kA$, are maintained, resulting in approximately the same plasma density evolution in (c) for all three shots. One can see the plasma locking in (d) when the $n = 1$ RWM/EF coil currents in (e) are increased up to each threshold, as seen in shots marked by red and blue. An important observation in these experiments is the change in the threshold, depending on β_N. The β_N is the critical parameter for plasma stability, and so for plasma responses. The β_N in (b) is produced differently in experiments by differing NBI power, for example, $3MW$ for black and blue traces, and $2MW$ for red traces. One

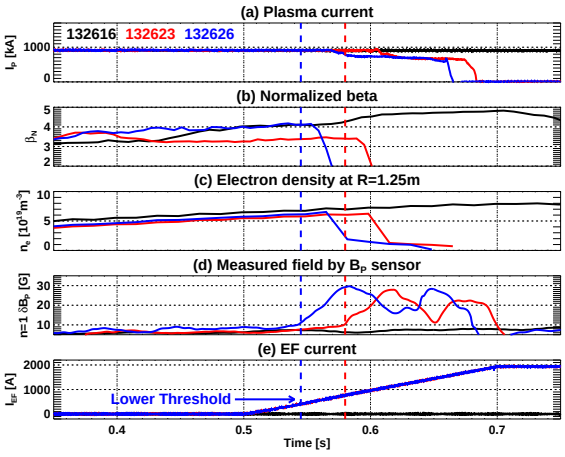

FIG. 3. Time trace of typical locking experiments in this study, including each (a) plasma current, (b) β_N, (c) electron density, (d) $n = 1$ signal, and (e) applied currents for $n = 1$ field. The black traces are for reference discharge, and the red and blue traces are for the low $\beta_N \sim 3$ and the high $\beta_N \sim 4$. One can see the smaller threshold for the higher β_N as indicated by dot lines at the time of locking.

can see clearly from the blue traces that the threshold is reduced and thus locking occurs earlier for higher β_N. This trend, as summarized in Figure 4, has been observed in JET experiments [4] and also in recent DIII-D experiments. The greater sensitivity of plasmas to error field has been predicted in fact theoretically [17] by Resonant Field Amplification (RFA), which describes the increase of the plasma response when plasma approaches to a marginal stability, $\beta_N \rightarrow \beta_{N,marginal}$. Note that our experiments are designed not to hit the actual marginal limit, since then Resistive Wall Mode (RWM) can play an important role.

Results imply that plasma response becomes stronger for higher β_N, and thus the lower external field is required to produce the same electromagnetic torque. On the other hand, the compensating mechanism against the electromagnetic torque arises through the viscous torque, which is tightly associated with the rotation but empirically seems to appear as the positive density correlation. So empirically the higher external threshold is expected for the higher plasma density, which is typically accompanied with higher β_N plasmas. However, this prediction fails due to plasma response effects. Figure 5 shows the external current threshold versus the line-averaged plasma density, combining previous Ohmic experiments (Black diamond) and present high β experiments (Red circle). One can see the almost linear correlation for Ohmic experiments, but the correlation is no longer valid for high β cases.

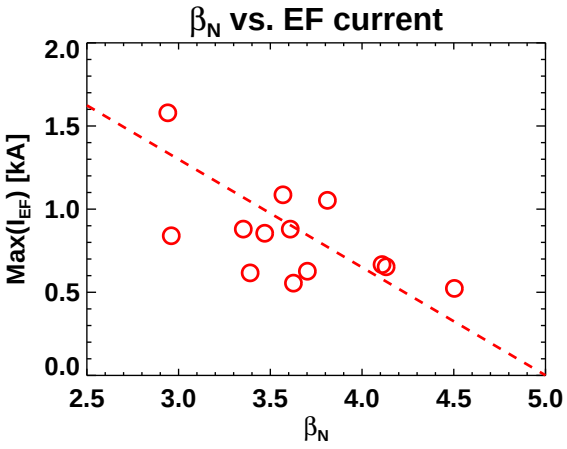

FIG. 4. Summary of experimental observations for the error field threshold in external currents vs. β_N. One can find the greater sensitivity of plasmas to higher-β_N plasmas.

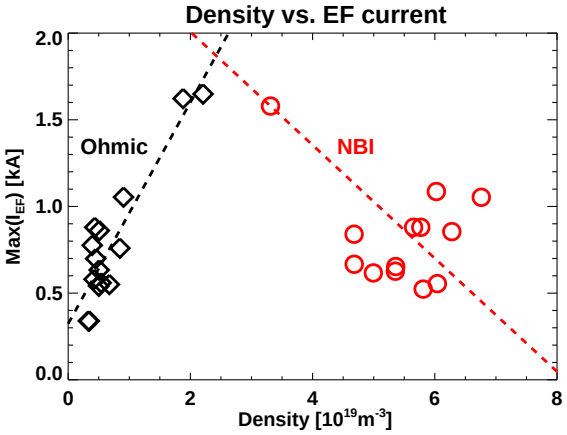

FIG. 5. Summary of locking threshold measurements in external currents vs. density for NBI-heated high β cases (Red circle) including Ohmic plasma cases (Black diamond). The linear density correlation in Ohmic plasmas is no longer valid for high β plasmas when the external measures are used.

In fact, one can see the opposite correlation for high β cases roughly as well as the large discrepancy between Ohmic cases [8] and high β cases. It is found that the linear correlation can be restored if the total resonant field including plasma response is used for threshold instead of external current or external resonant field, as will be discussed in details later.

It also worths mentioning that there are some effects by intrinsic error field in our experiments. In most of shots, the toroidal phase of EFC currents is designed to be approximately aligned with the intrinsic error field, to reduce the currents we need to apply. In order to

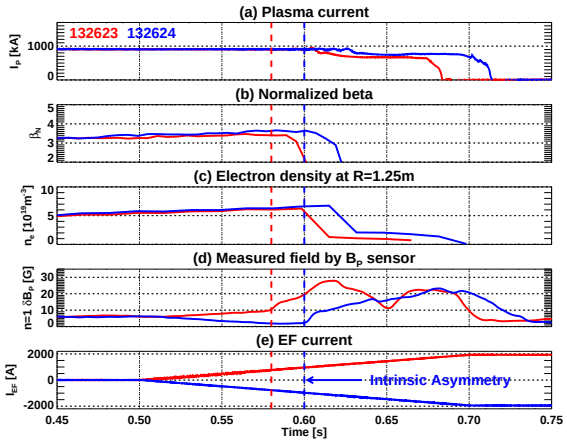

FIG. 6. Time trace of locking experiments indicating the intrinsic error field, including each (a) plasma current, (b) β_N, (c) electron density, (d) $n = 1$ signal, and (e) applied currents for $n = 1$ field. The field in the blue traces is identical but different by 180° toroidal phase, compared to the red traces. The large threshold in the blue traces implies that the intrinsic error field exists and is compensated by the applied field.

ensure this, several shots used the opposite toroidal phase of EFC currents, as shown in an example, Figure 6. One can see the blue traces caused locking later with larger threshold, which implies in this case that the applied field is compensating intrinsic error field. The difference in FEC currents is about $\sim 200A$, and thus effects by intrinsic error field in our experiments are $10 \sim 20\%$.

Another set of experiments was designed to study the role of plasma rotation, which can be directly measured by CHERS in NBI-heated plasmas, unlike Ohmic plasmas. We used magnetic braking to change rotation, as the $n = 3$ components of 3D fields can be produced independently of the $n = 1$ components. Plasmas with a braking may be not identical to plasmas without a braking even if the same rotation profile is achieved, but our experiments ignored such possible differences. A typical example is shown in Figure 7. Three different shots represent a reference (black), a shot with the only $n = 1$ (red) and a shot with the $n = 1$ and $n = 3$ field. Almost identical conditions, as shown in (a) plasma currents and (b) densities, are produced except (c) rotations, however by utilizing different 3D fields with (e) the $n = 1$ and (f) the $n = 3$ to find different thresholds in (d). In the shot with the $n = 3$ braking (blue), one can see the lower level of rotation was maintained. As a result, the locking threshold measured by the $n = 1$ currents becomes lower, by a factor of 2 in this

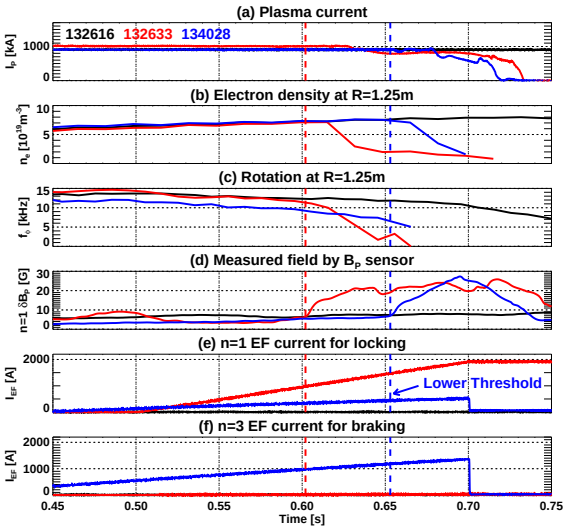

FIG. 7. Time trace of locking experiments with the $n = 3$ rotation braking, including each (a) plasma current, (b) β_N, (c) electron density, (d) $n = 1$ signal, (e) applied currents for $n = 1$ field, and (f) applied currents for $n = 3$ field. The black traces are for reference discharge, and the red and blue traces are for the high β discharges but only the blue traces have the $n = 3$ braking and thus different rotation. One can see the increased sensitivity when rotation is low.

case.

The positive correlation between the threshold and the rotation, illustrated in Figure 7 can be easily predicted by theory as the rotation would increase viscous torque compensating against electromagnetic torque. However, it has been rather implicit in the traditional locking scaling due to difficulties to measure the rotation profile evolutions in Ohmic plasmas, during a short period of time during the locking process. Instead, the correlation with the density has been used since it appears to be very strong and robust. This density correlation is not yet fully resolved in the theory. Only a theory by Cole showed a possible role of Neoclassical Toroidal Viscosity (NTV) [23] since then the linear density scaling could be obtained. The validation of this theory remains as the future work. The primary focus of this paper is on the role of plasma response to explain Ohmic and high β results consistently, with a conventional scaling such as the density scaling, but the effect of rotation on error field threshold is obvious as seen in Figure 7 and cannot be ignored.

III. THEORY: AMPLIFICATION THROUGH PLASMA COUPLING

Error fields produce plasma response along with perturbed plasma currents, which often largely distort field penetration. Therefore, plasma response should be considered to determine actual resonant field driving islands and locking. Plasma response is important even in Ohmic plasmas as found in NSTX and DIII-D [9, 13, 14], but perhaps plays more important role in high β plasmas due to larger amplification of the field. Figures 4 already implies the importance of plasma response and amplification, as it can be understood that the threshold decreases because plasma approaches to marginal β_N limit and thus plasma response increases.

When one studies the error field threshold including plasma response effects, one needs to define a field component that can relevantly describe or dominate locking dynamics. It has been traditional to define this as the 2/1 resonant component, δB_{21}, since locking mostly appears to be directly related to magnetic island activities at $q = 2/1$ surface as discussed in Introduction, and δB_{21} determines the size of magnetic islands. One can calculate this in terms of external (vacuum) field, δB^x_{21} by ignoring plasma response and assuming a full penetration, or one can calculate this by including perturbed plasma current effects, $\delta B_{21} = \delta B^x_{21} + \delta B^p_{21}$. As shown in the previous work [9, 14], the external resonant field δB^x_{21} often fails, and the total resonant field δB_{21} with ideal plasma response better addresses locking physics and experimental observations.

Figure 8 is the revision of Figure 5, using the total resonant fields calculated by Ideal Perturbed Equilibrium Code (IPEC) [25], instead of external currents or external fields. Compared to Figure 5, the difficulty to observe any correlation in terms of external currents can be resolved, as the linear correlation appears again consistently for both Ohmic and NBI-heated plasmas. This resolution comes from plasma amplifications by a factor of $2-3$ in high density and high β plasmas, as briefly reported in recent NSTX overview paper [24]. Note that these calculations of total resonant fields included the contributions from the intrinsic error field by the center-stack distortion and PF5 non-circularity. These contributions are not significant, but not ignorable, as demonstrated in Figure 6.

The actual scaling of error field threshold should include other parameters as well as the density. Previous work has shown the strong correlation with plasma density n_e, toroidal field B_{T0}, and major radius R_0 [3–6, 8]. Many global parameters were investigated, and this

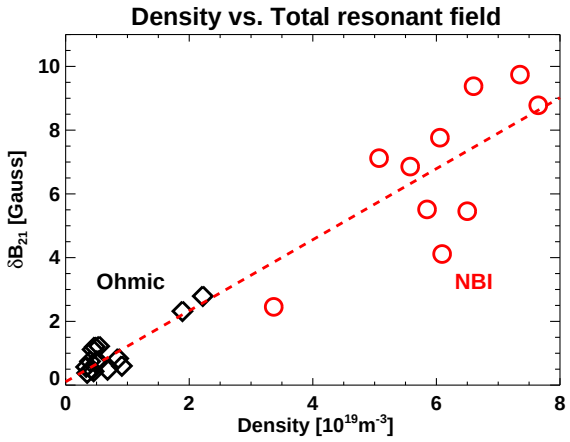

FIG. 8. Revision of Figure 5, using total resonant fields at $q = 2/1$ surface instead of external currents. Ideal Perturbed Equilibrium Code (IPEC) is used for these calculations. One can see that the density correlation is now restored consistently for both Ohmic and NBI-heated plasmas. This is due to large plasma amplifications in high β plasmas as briefly reported by Figure 3, in recent NSTX overview paper [24].

study also found n_e and B_{T0} are most important variables. The major radius is not relevant here since experiments are limited in NSTX configuration, but it is still important to ensure that our scaling is dimensionless and independent of size. Based on the Connor-Taylor invariance [26], $n_e R_0^2$ and $B_{T0} R_0^{5/4}$ is used for scaling instead of mere n_e and B_{T0}.

In NSTX, there exists an additional parameter showing significant correlation. It is the shear in q-profiles, and this scaling has already been found in the previous study for NSTX Ohmic plasmas [8]. This q-shear is in fact very natural if one notes the size of magnetic islands is inversely proportional to $dq/d\psi$. Since higher fields are required to open the same size of islands when the $dq/d\psi$ is higher, so the positive correlation in the threshold is naturally expected as found in the previous study. The q-shear scaling has not been clearly shown in other studies in other devices, but possibly it is due to the limited range of the q-profiles in experiments. In fact, DIII-D has reported the different scaling for different q_{95}'s, although sometimes the effects by q-profiles were not clearly separable from B_{T0} [9].

Resulting scaling is presented in Figure 9. One can see that Ohmic (Black diamond) and high β (Red circle) results are well combined by one scaling with reasonably small deviations, which are not found when the external resonant fields are used. Including proportional

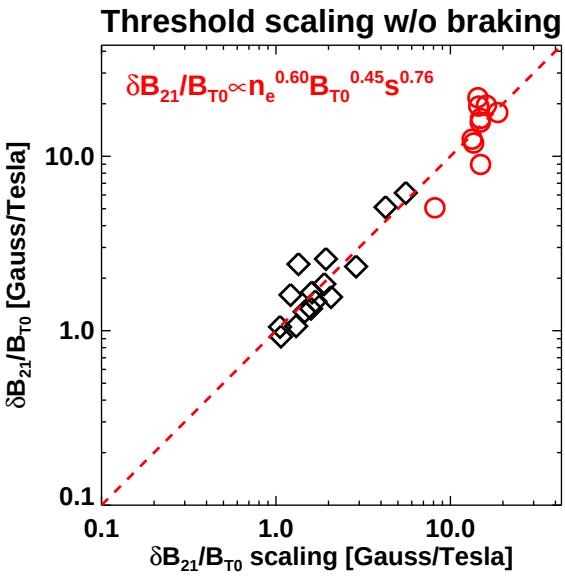

FIG. 9. Error field threshold scaling by the total resonant fields including Ohmic (Black diamond) and high β (Red circle) cases. Note that the scaling can be improved from Figure 8 by including additional parameters such as B_{T0} and the shear at the $q = 2/1$ surface, s. The density correlation becomes weaker than the almost linear correlation in Ohmic plasmas.

factors, error field threshold in NSTX is given by

$$\left(\frac{\delta B_{21}}{B_{T0}}\right) \cong 2.2 \times 10^{-4} n_e^{0.60} B_{T0}^{0.45} s^{0.76} R_0^{1.74}, \tag{1}$$

where the shear is defined as $s \equiv dq/d\rho$ at $q = 2/1$, with the $\rho \equiv \sqrt{\psi_N}$. The density correlation is weaker quite significantly than the linear correlation when including high β cases, and this aspect will be discussed in the next Section. One can also compare this with the previous Ohmic results, $\delta B_{21}/B_{T0} \propto n_e^{0.88} B_{T0}^{0.23} s^{0.79}$ in Ref. [8], where the density correlation is closer to the linear correlation. The major radius scaling appears to be strong, but here this is just the result of Connor-Taylor constraint and should not be taken as a robust parameter unless larger devices are tested and included in scaling.

IV. DISCUSSION: EFFECTS BY PLASMA ROTATION

The weaker density correlation can be understood due to the additional drive of the torque in high β cases by NBI heating. In other words, the torque implication by the density can be possibly weaker in NBI-heated plasmas. However, it would predict that the

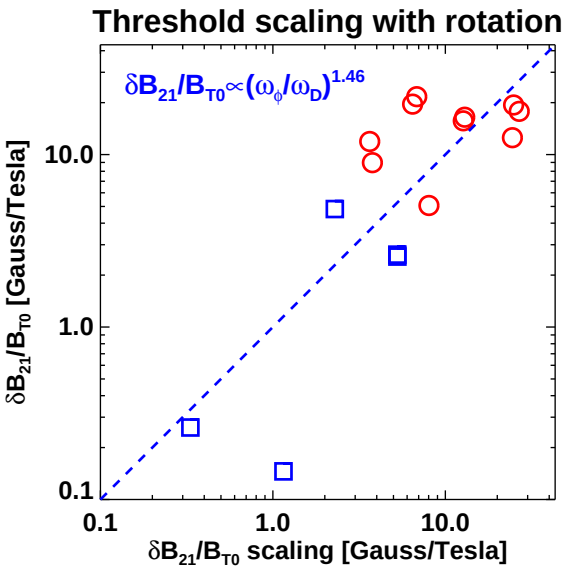

FIG. 10. Error field threshold scaling with the rotation, including high β cases with (Blue square) and without (Red circle) magnetic braking. The correlation between the field threshold and the rotation is strong as expected.

threshold increase rather than the decrease in the same density, since the additional torque drive should be compensating to error field. The decrease for the density power index may imply that our NBI heating is slightly more effective to increase the density rather than the torque or the rotation. The density increases by up to a factor of ~ 10 compared to Ohmic plasmas, and indeed the rotation increase by a factor of ~ 10 from Ohmic to high β plasmas is unlikely.

The rotation is an attractive parameter than the density for scaling, by its direct implication on the viscous torque. However, the experimental information for the rotation is available only for NBI-heated cases. Also, effects by the rotation and the density are not clearly separable, and the interlink between the two parameters are not that simple since their contributions to the electromagnetic torque or the viscous torque are coupled [12]. It is found when both the rotation and the density are included simultaneously, their effects are largely duplicated and the regression analysis is performed with ill-conditions. Therefore, our approach is to hold the scaling in Figure 9, but to consider effects by rotation as a correction. For a dimensionless variable, the ratio of the toroidal rotation to the diamagnetic rotation at the $q = 2/1$ is chosen.

Figure 10 shows the resulting scaling in high β cases, with the rotation as a correction.

Although the standard deviations are increased, it represents well high β experiments with and without magnetic braking. With the proportional factors, the error field threshold in NSTX high β cases is given by

$$\left(\frac{\delta B_{21}}{B_{T0}}\right)_{\omega} \cong \left(\frac{\delta B_{21}}{B_{T0}}\right) \times \left(0.22\frac{\omega_{\phi}}{\omega_{D}}\right)^{1.46}. \tag{2}$$

The correlation with the rotation is strong as expected, and indicates that the error field sensitivity would increase faster than the linear when the rotation decreases. The proportional factor 0.22 is interesting, since this implies that the scaling without magnetic braking in Figure 9 can be restored if $\omega_{\phi} \sim 4.5 \times \omega_{D}$. That is, Equation (1) and (2) can be consistent when the actual rotation higher than ω_{D} by a factor of $4 \sim 5$.

V. SUMMARY

This paper presented various $n = 1$ locking experiments in NSTX high β plasmas, with and without $n = 3$ magnetic braking. It is shown that plasmas have the greater sensitivity in higher β plasmas due to plasma amplification. Error field threshold becomes lower, which is seemingly inconsistent with Ohmic threshold scaling which predicts the higher threshold in high density and high β. This can be resolved by considering the total resonant field including plasma response and amplification, and the resulting scaling becomes consistent for both Ohmic and high β plasmas. The sensitivity can be greater if the rotation is decreased by reducing input torques by magnetic braking. The strong correlation is indeed found between the error field threshold and the rotation as predicted. Resulting scaling may be helpful for ITER, but the actual extrapolation to ITER is not discussed here since the extrapolation will be more relevant when these data are combined with other tokamaks, as planned for the future work. Nevertheless, this scaling will be useful specifically for Spherical Torus (ST) including future devices such as NSTX-Upgrade.

ACKNOWLEDGMENTS

This work was supported by DOE contract DE-AC02-76CH03073 (PPPL), DE-FC02-04ER54698 (GA), and DE-FG02-03ERS496 (CU).

---

[1] T. C. Hender, R. Fitzpatrick, A. W. Morris, P. G. Carolan, R. D. Durst, T. Eddlington, J. Ferreira, S. J. Fielding, P. S. Haynes, J. Hugill, I. J. Jenkins, R. J. La Haye, B. J. Parham, D. C. Robinson, T. N. Todd, M. Valovic, and G. Vayakis, Nucl. Fusion **32**, 2091 (1992).

[2] R. J. La Haye, R. Fitzpatrick, T. C. Hender, A. W. Morris, J. T. Scoville, and T. N. Todd, Phys. Fluids B **4**, 2098 (1992).

[3] R. J. Buttery, M. D. Benedetti, D. A. Gates, Y. Gribov, T. Hender, R. J. La Haye, P. Leahy, J. A. Leuer, A. W. Morris, A. Santagiustina, J. T. Scoville, B. J. D. Tubbing, the JET Team, the COMPASS-D Research Team, and the DIII-D Team, Nucl. Fusion **39**, 1827 (1999).

[4] R. J. Buttery, M. D. Benedetti, T. C. Hender, and B. J. D. Tubbing, Nucl. Fusion **40**, 807 (2000).

[5] J. T. Scoville and R. J. LaHaye, Nucl. Fusion **43**, 250 (2003).

[6] S. M. Wolfe, I. H. Hutchinson, R. S. Granetz, J. Rice, A. Hubbard, A. Lynn, P. Phillips, T. C. Hender, D. F. Howell, R. J. La Haye, and J. T. Scoville, Phys. Plasmas **12**, 056110 (2005).

[7] D. F. Howell, T. C. Hender, and G. Cunningham, Nucl. Fusion **47**, 1336 (2007).

[8] J. E. Menard, R. E. Bell, D. A. Gates, S. P. Gerhardt, J.-K. Park, S. A. Sabbagh, J. W. Berkery, A. Egan, J. Kallman, S. M. Kaye, B. LeBlanc, Y. Q. Liu, A. Sontag, D. Swanson, H. Yuh, W. Zhu, and the NSTX Research Team, Nucl. Fusion **50**, 045008 (2010).

[9] J.-K. Park, M. J. Schaffer, R. J. La Haye, T. J. Scoville, and J. E. Menard, Phys. Plasmas **51**, 023003 (2011).

[10] R. Fitzpatrick and T. C. Hender, Phys. Fluids B **3**, 644 (1991).

[11] R. Fitzpatrick, Nucl. Fusion **33**, 1049 (1993).

[12] A. J. Cole and R. Fitzpatrick, Phys. Plasmas **13**, 032503 (2006).

[13] J.-K. Park, M. J. Schaffer, J. E. Menard, and A. H. Boozer, Phys. Rev. Lett. **99**, 195003 (2007).

[14] J.-K. Park, A. H. Boozer, J. E. Menard, A. M. Garofalo, M. J. Schaffer, R. J. Hawryluk, S. M. Kaye, S. P. Gerhardt, S. A. Sabbagh, and the NSTX team, Phys. Plasmas **16**, 056115 (2009).

[15] H. Reimerdes, A. M. Garofalo, E. J. Strait, R. J. Buttery, M. S. Chu, Y. In, G. L. Jackson, R. J. La Haye, R. J. Lanctot, Y. Q. Liu, M. Okabayashi, J.-K. Park, M. J. Schaffer, and W. M. Solomon, Nucl. Fusion **49**, 115001 (2009).

[16] M. J. Lanctot, H. Reimerdes, A. M. Garofalo, M. S. Chu, Y. Q. Liu, E. J. Strait, G. L. Jackson, R. J. La Haye, M. Okabayashi, T. H. Osborne, and M. J. Schaffer, Phys. Plasmas **17**, 030701 (2010).

[17] A. H. Boozer, Phys. Rev. Lett. **86**, 5059 (2001).

[18] A. C. Sontag, S. A. Sabbagh, W. Zhu, J. M. Bialek, J. E. Menard, D. A. Gates, A. H. Glasser, R. E. Bell, B. P. LeBlanc, M. G. Bell, A. Bondeson, J. D. Callen, M. S. Chu, C. C. Hegna, S. M. Kaye, L. L. Lao, Y. Liu, R. Maingi, D. Mueller, K. C. Shaing, D. Stutman, and K. Tritz, Phys. Plasmas **12**, 056112 (2005).

[19] S. A. Sabbagh, A. C. Sontag, J. M. Bialek, D. A. Gates, A. H. Glasser, J. E. Menard, W. Zhu, M. G. Bell, R. E. Bell, A. Bondeson, C. E. Bush, J. D. Callen, M. S. Chu, C. C. Hegna, S. M. Kaye, L. L. Lao, B. P. LeBlanc, Y. Q. Liu, R. Maingi, D. Mueller, K. C. Shaing, D. Stutman, K. Tritz, and C. Zhang, Nucl. Fusion **46**, 635 (2006).

[20] A. Sontag, S. Sabbagh, W. Zhu, J. Menard, R. Bell, J. Bialek, M. Bell, D. Gates, A. Glasser, B. LeBlanc, K. Shaing, D. Stutman, and K. Tritz, Nucl. Fusion **47**, 1005 (2007).

[21] M. G. Bell, R. E. Bell, D. A. Gates, S. M. Kaye, H. Kugel, B. P. LeBlanc, F. M. Levinton, R. Maingi, J. E. Menard, R. Raman, S. A. Sabbagh, D. Stutman, and the NSTX team, Nucl. Fusion **46**, S565 (2006).

[22] J. E. Menard, R. E. Bell, D. A. Gates, S. M. Kaye, B. P. LeBlanc, F. M. Levinton, S. S. Medley, S. A. Sabbagh, D. Stutman, K. Tritz, and H. Yuh, Phys. Rev. Lett. **97**, 095002 (2006).

[23] A. J. Cole, C. C. Hegna, and J. D. Callen, Phys. Rev. Lett. **99**, 065001 (2007).

[24] R. Raman, J.-W. Ahn, J. P. Allain, R. Andre, R. Bastasz, D. Battaglia, P. Beiersdorfer, M. Bell, R. Bell, E. Belova, J. Berkery, R. Betti, J. Bialek, T. Bigelow, M. Bitter, J. Boedo, P. Bonoli, A. Boozer, A. Bortolon, D. Brennan, J. Breslau, R. Buttery, J. Canik, G. Carravelli, C. Chang, N. A. Crocker, and D. Darrow, Nucl. Fusion **51**, 094011 (2011).

[25] J.-K. Park, A. H. Boozer, and A. H. Glasser, Phys. Plasmas **14**, 052110 (2007).

[26] J. W. Connor and R. J. Hastie, Nucl. Fusion **13**, 221 (1973).

LIST OF FIGURES

The Princeton Plasma Physics Laboratory is operated
by Princeton University under contract
with the U.S. Department of Energy.

Information Services
Princeton Plasma Physics Laboratory
P.O. Box 451
Princeton, NJ 08543

Phone: 609-243-2245
Fax: 609-243-2751
e-mail: pppl_info@pppl.gov
Internet Address: http://www.pppl.gov